Plasma gradient controlled injection and postacceleration of high quality electron bunches

C.G.R. Geddes[*], E. Cormier-Michel[*], E. Esarey[*,†], K. Nakamura[*], G.R. Plateau[*,**], C.B. Schroeder[*], Cs. Toth[*], D.L. Bruhwiler[‡], J.R. Cary[‡,§] and W.P. Leemans[*,¶]

[*]*Lawrence Berkeley National Laboratory, 1 Cyclotron Rd, Berkeley CA 94720*
[†]*Also at U. Nevada, Reno*
[**]*Also at École Polytechnique, France*
[‡]*Tech-X Corporation, 5621 Arapahoe Ave. Ste. A, Boulder CO 80303*
[§]*Also at U. Colorado, Boulder*
[¶]*Also at U. Nevada, Reno and U.C. Berkeley*

Abstract. Plasma density gradient control of wake phase velocity and trapping threshold in a laser wakefield accelerator produced electron bunches with absolute longitudinal and transverse momentum spreads more than ten times lower than in previous experiments (0.17 and 0.02 MeV/c FWHM, respectively) and with central momenta of 0.76 $\pm$ 0.02 MeV/c, stable over a week of operation. Simulations validated against diagnostics show that use of such bunches as a wakefield accelerator injector can produce stable beams with 0.2 MeV/c-class momentum spread at high energies. Preservation of bunch momentum spread requires high simulation momentum accuracy, and related self-trapped simulations showed that high order particle weight effectively suppresses simulation momentum errors allowing design of low emittance stages.

Keywords: Laser Wakefield Acceleration, Plasma Gradient Controlled Injection, Particle in Cell Simulation
PACS: 52.38.Kd, 41.75.Jv, 29.25.Bx

INTRODUCTION

Laser wakefield accelerators (LWFAs) [1] have demonstrated acceleration to GeV energies in a few cm [2], reducing accelerating distances by a thousandfold compared to conventional technologies. The laser ponderomotive (radiation) pressure drives a plasma density wave (wake), whose longitudinal field can "self-trap" and accelerate electrons from the plasma [1, 3]. Recently, self trapped experiments produced bunches with few MeV/c momentum spreads near 100 MeV/c by extending the laser propagation distance using a guiding channel [4] or large spot size [5, 6]. Channel guided LWFAs subsequently produced bunches with $\sim$ 20 MeV/c longitudinal and 2 MeV/c transverse momentum spread at 1 GeV and stable bunches at 500 MeV [2, 7] .

In self-trapped experiments, injection, acceleration, and guiding are interdependent, limiting tunability. Beam quality was best when operating at the trapping threshold [5, 6, 7, 8], and relatively stable operation [2, 7, 9] was only observed in a narrow parameter window. The plasmas used had approximately constant density along the laser propagation direction, so that the wake phase velocity v_ϕ was $\sim v_g$ (the laser group velocity [3]). Using lower plasma density increases v_g and hence v_ϕ, allowing electrons to

CP1086, *Advanced Accelerator Concepts: 13th Workshop,* edited by C. B. Schroeder, W. Leemans, and E. Esarey
© 2009 American Institute of Physics 978-0-7354-0617-9/09/$25.00

accelerate to higher energies while remaining in phase with the wake [5, 6, 2]. However no self-trapping is observed for given laser parameters below a minimum density [5, 6, 2] indicating the need for externally controlled injection.

Independent control over electron injection into the wake and of the accelerating structure could increase bunch energy by allowing operation of the accelerator at lower density, while also improving stability and quality by allowing independent tuning of injection. This is important for many applications, which desire momentum spreads below those of present experiments (1-20 MeV/c or few % longitudinal spread and ~0.2-2 MeV/c transverse spread). The short plasma wave wavelength, $\lambda_p = \sqrt{\pi c^2 m/e^2 n_e}$ typically $\sim 10-100$ μm, determines the size requirement for the injected bunch. Here n_e is the plasma density, e and m the electron mass and charge, and c the speed of light. Experiments [10] have demonstrated controlled injection using the colliding laser pulse method [11, 12, 13] showing that controlled injection allows tuning the electron bunch energy by changing the injection location within the plasma, but further reduction in momentum spread is still desired.

Plasma density gradients with density decreasing in the laser propagation direction (downramps) have been proposed to control trapping. In such gradients λ_p increases with propagation, causing the wake fronts behind the laser to fall further behind as the laser propagates which decreases the wake phase front velocity v_ϕ [14, 15, 16, 17]. Use of the gradient separates density (which controls resonance of the plasma wave with laser pulse length [3]) from wake phase velocity, and controls wake phase velocity as a function of propagation distance. The reduced v_ϕ reduces the threshold for trapping by reducing the velocity electrons must achieve to be trapped, and hence allows trapping at lower densities than in uniform plasmas. Such tuning of the trapping threshold has been shown to produce stable electron bunches with an order of magnitude lower absolute momentum spread than other LWFA experiments [18]. The reduced phase velocity also reduces the maximum energy gain however because dephasing occurs quickly. Hence for stable high energy bunches a downramp region to control trapping should be followed by a long uniform-density plasma for acceleration to high energy.

Here, we report that using plasma density gradient controlled trapping produced bunches with an order of magnitude lower absolute momentum spread than previous experiments, and show that the bunches were stable over a week of operation and hundreds of shots. Electron bunches at momenta of 0.76 MeV/c and with 0.17 MeV/c FWHM momentum spread, 0.02MeV/c central momentum stability and transverse momentum, and 2 mrad (0.002 MeV/c) RMS pointing stability over hundreds of shots were produced with hundreds of pC of charge. Simulations, validated in detail against experimental diagnostics, show these bunches can be used as an LWFA injector for stable low energy spread bunches at high energy as needed for applications. High order particle weight is shown to be important for PIC simulation of such low momentum spread bunches.

The experimental setup is displayed in Fig. 1, showing a pulse from the LOASIS Ti:Sapphire laser [19] focused on the downstream edge of a thin slit gas jet oriented transversely to the laser axis. The laser ionized the hydrogen gas and drove a plasma wake. Peak laser power was 10 TW (0.5 J in 47 fs FWHM), focused to a 7.5 μm FWHM spot. The plasma density profile in the laser propagation direction was measured to be Gaussian for densities above the interferometer measurement threshold of

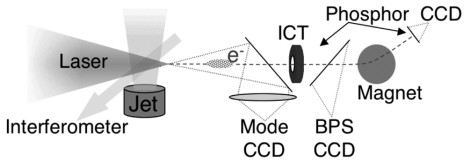

FIGURE 1. (color). Setup for density gradient controlled injection. The laser was focused at the downstream edge of a thin slit gasjet where the density is decreasing. An interferometer measured the plasma profile. Electron diagnostics include a magnetic spectrometer, bunch phosphor screen and ICT.

$\sim\ 2\times\ 10^{18}$ cm^{-3}, with a peak density of 2.2 $\pm 0.3\times 10^{19}$ cm^{-3} and a FWHM of 750 μm ± 100 μm. The wake is excited strongly within a Rayleigh range $Z_R \sim 200$ μm of the laser focus [3], a small fraction of the jet length. This allowed effective selection of the density gradient where the wake is excited, and hence control of trapping, using laser focus location [18]. Focusing upstream of the jet center produced an increasing or flat density, published previously [8], while focusing downstream produced a decreasing density. Electron bunches were characterized by a magnetic spectrometer. The bunch was bent 55° onto a phosphor screen (LANEX) imaged by a CCD, which imaged a momentum range of $\pm 14\%$ about a central momentum determined by the magnet current. Momentum resolution was $\pm 5\%$. Beam divergence was observed in the out-of-plane direction. Alternatively, divergence and profile in both planes was observed by an insertable bunch phosphor screen (BPS). Charge was determined by cross-correlating the phosphor signals with an integrating current transformer (ICT). Transmitted laser mode and THz bunch length measurements were presented in [18].

Focusing at the downstream edge of the jet, in the density downramp, produced electron bunches with an order of magnitude lower absolute momentum spread and jitter than previously observed in LWFAs [18] and multiple datasets on different run days showed that accelerator operation was stable and repeatable over a week of operation.

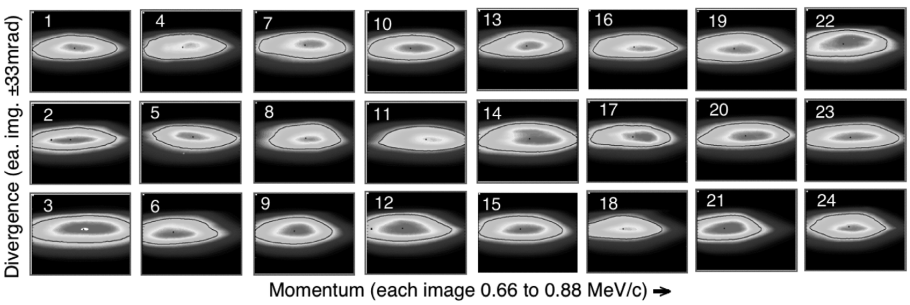

FIGURE 2. (color). Sequential magnetic spectra with the laser focus in the density downramp, from dataset A, display stable bunch performance (showing the 24 shots with the same magnet setting out of the 45 shots in this sequence).

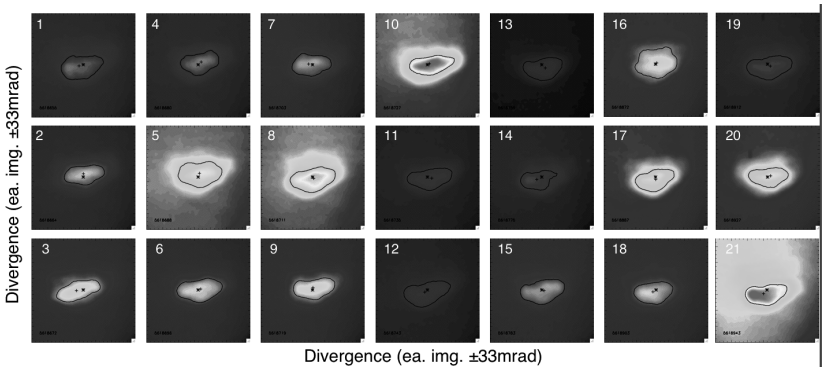

FIGURE 3. (color). Sequential electron bunch profiles with the laser focus in the density downramp, from dataset A. The black solid contour indicates the small-divergence feature (70% of peak). The + indicates the centroid of this feature relative to the mean centroid over all shots (*). Images are plotted on a fixed scale to show charge stability (showing 21 of the 31 shots in this sequence).

Magnetic spectrometer dataset A (Fig. 2) showed bunches with central momentum stable at 0.76 MeV/c $\pm$0.02 MeV/c RMS and with momentum spread stable at 0.17 MeV/c FWHM (20 %) $\pm$ 0.02 MeV/c RMS over 28 sequential and 45 total diagnostic shots. In the undispersed plane, the bunch divergence was 20 mrad FWHM $\pm$ 1.8 mrad RMS, and pointing deviation was 1.5 mrad RMS.

Bunch divergence in both planes (momentum integrated) was measured on the insertable BPS phosphor (Fig. 3) [20]. A small-divergence bunch is visible surrounded by a broad background. The small-divergence feature has a divergence of 26 (14) mrad in the horizontal (vertical) plane with RMS deviations of $\pm$1.8 (2.5) mrad over 31 shots. Bunch pointing showed 1.8 (1.2) mrad RMS and 8 (5) mrad peak-to-peak deviations in the horizontal (vertical) plane. Deviations in pointing and divergence are much less than the beam divergence. Vertical data agree with measurements from the magnetic spectrometer, indicating that the narrow feature is the MeV bunch. The broad background is likely lower momentum electrons. The observed divergence indicates transverse bunch momenta of $\sim$ 0.02 MeV/c, much lower than the 0.3-2 MeV/c in conventional self-trapped experiments [4, 2].

The signals on the magnetic spectrometer and the narrow divergence feature on the BPS phosphor were correlated to ICT charge measurements to extract the charge of the bunch at 0.76 MeV/c. This gave Q_{bunch} of 0.3 - 1 nC. Charge stability was 40% RMS in this dataset.

Central momentum was stable between 0.76 and 0.78 MeV/c, FWHM energy spread between 0.16 and 0.19 MeV/c, and divergence between 17 to 23 mrad over three runs and over a week of clock time. Figure 4 shows data from a second sequence of 82 shots (set B), measured 123 hours after Fig. 2, demonstrating this stability. This will be important for LWFA applications and has not been previously observed. Charge stability as good as 15 % RMS was observed. Variation in charge stability from run to run is likely due to diurnal variation in laser stability and prepulse.

In the data presented in Figs. 2 and 4, a 10 μm silver coated nitrocellulose pellicle

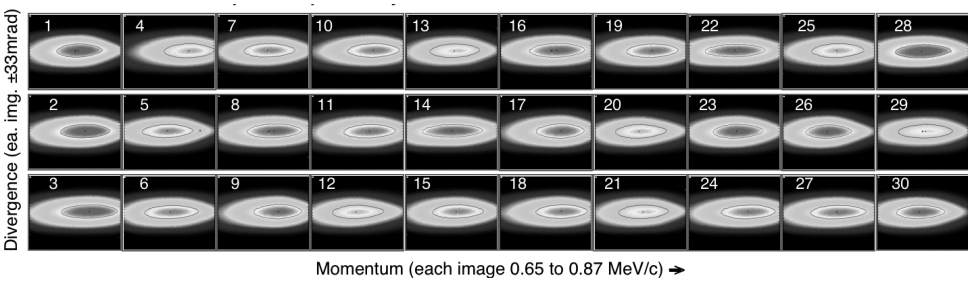

FIGURE 4. (color). Sequential magnetic spectra with the laser focus in the density downramp from run B, 123 hours after run A (showing 30 shots with the same magnet setting out of 82 shots in the sequence).

transmitted the electron bunch and diverted the laser to a mode imager CCD [21] to measure the laser profile at the plasma exit [18]. A third set of 60 shots (dataset C) taken immediately subsequent to that shown in Fig. 4 and with the mode imager pellicle removed, is displayed in Fig. 5. Visible is a reduction in FWHM divergence by $10-20\%$, and appearance of a narrow divergence feature (6 mrad) at the 80% contour, indicating that scattering contributed modestly to beam divergence in the measurements, and showing that there is a sub-population of electrons with lower divergence. Longitudinal momentum spread was not affected.

PIC simulations using the VORPAL [22] framework showed that the ramp decreased v_ϕ as described in [14], producing MeV-class electron bunches without significant plasma modulation of the laser. Simulated plasma density was 1.8×10^{19} cm^{-3} with a Gaussian profile of 900 μm FWHM, close to the experimental parameters. Consistent with experimental stability, simulations produced MeV-class bunches for laser powers of 8-10 TW and plasmas of 500-1000 μm FWHM with densities of $1.8-2.2\times10^{19}$ cm^{-3}. The laser focus was 600 μm downstream of the plasma center, in the range that produced MeV bunches experimentally. Because laser focusing through the jet required a large simulation domain of 400 μm (240 μm) in the longitudinal (transverse) direction,

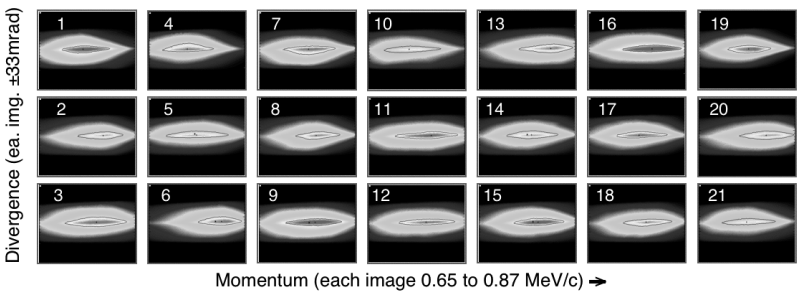

FIGURE 5. (color). Sequential magnetic spectra with the laser focus in the density downramp, and with the mode imager pellicle removed from the beam, from run C, the same day as run B (showing 21 shots with the same magnet setting out of the 60 shots in this sequence).

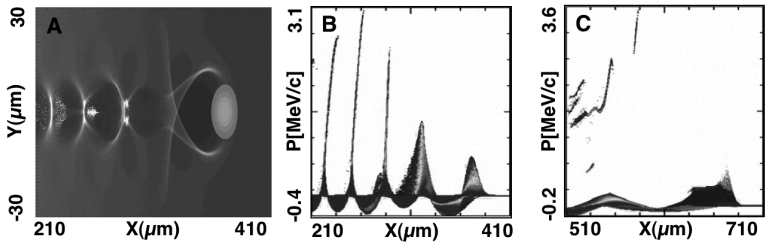

FIGURE 6. (color). Simulated wake and phase space. In the downramp, the structure of the wake (A) shows that the laser (red) drives a plasma density wake whose period varies as a function of distance behind the pulse (grey) in the downramp, trapping and accelerating electrons (yellow). Trapping of the electrons is shown in phase space (B) at the location of (A), and this bunch subsequently dephases due to the low wake velocity in the ramp, forming an ultrafast (<50 fs), narrow momentum spread bunch at an energy of 1.5 MeV/c (C).

simulations were conducted in 2D with 12,000 (900) cells and using 5 particles/cell. Tests indicated modulation of the laser pulse was a small effect, allowing the laser to be launched 750 μm into the ramp to keep the simulation domain size tractable. An electron bunch was trapped at a density of $\sim 5 \times 10^{17}$ cm^{-3}, where the laser pulse length was resonant with λ_p (Fig. 6). At this density no trapping occurs in a homogeneous plasma because of high v_ϕ , emphasizing the ramp's effect. Particles were trapped and accelerated to $\sim$ 1.5 MeV/c (Fig. 6) with an absolute momentum spread of $<$ 0.2 MeV/c, similar to the experimental observation. Relative momentum spread in simulations and experiments was at the $10-20\%$ level, consistent with other simulations and experiments far above trapping threshold [2]. These results have now been reproduced using the VORPAL envelope model [23, 24], which is now being used to conduct larger scale and 3D simulations to resolve remaining discrepancies with experiments.

The simulations observed beam transverse momentum of $\sim$0.05 MeV/c, or divergence of 30 mrad, comparable to experimental measurements of 20 mrad. Simulations demonstrated that the low transverse momentum resulted because the low trapping threshold produced by the downramp decreased the transverse wake fields at trapping. This is in contrast to simulations and experiments in homogeneous plasmas, where strong transverse wakefields have been shown to result in transverse wave breaking, imparting much higher transverse momenta of 0.3-2 MeV/c to the bunch [25, 26]. The low transverse bunch momentum reduces normalized emittance. Using the simulated bunch size of $\sim$10 μm long by 5 μm diameter, we obtain $\varepsilon_n \sim 0.2-0.4\ \pi$ mm-mrad. In principle, this data indicates that emittance can be further improved using sharper gradients to further reduce the transverse field contributions.

The low phase velocity which stabilizes and controls trapping also causes rapid dephasing of the electron bunch, setting the 1 MeV-class maximum energy observed, and requiring injection of these bunches into a subsequent LWFA stage to achieve high energy. As λ_p lengthens in the downramp, the bunch expands to ≥ 50 μm in dimension, and this length has been benchmarked to THz radiation measurements [27]. Use of the bunches as an injector therefore requires that the post-accelerating stage be directly coupled to the downramp at the dephasing point, so that the bunch remains smaller than

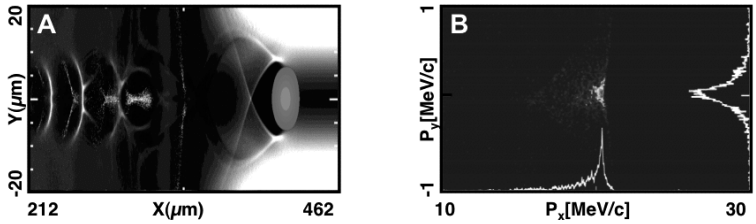

FIGURE 7. (color). Simulations merging density gradient injection to an accelerating channel at the location where the electrons dephase in the downramp (C in fig. 6). A continuous wake is driven (A) across the transition from the ramp into the channel (plasma wake density, grey) by the laser (red) accelerating particles (yellow). Acceleration in the channel (B) produces 20 MeV bunches while preserving the 0.2 MeV/c momentum spread.

λ_p. Use of such a continuous plasma in turn requires that the laser be well transmitted through the downramp to drive the wake for postacceleration. Experiments [27, 18] and simulations (Fig. 6) show that this requirement is met. The transmitted laser mode was similar to the vacuum mode, with no filamentation and with laser transmission of more than 70% when the jet was preionized by an 'ignitor' laser pulse arriving before the drive pulse (ignitor setup shown in [21]).

Simulations ending the downramp in a plasma channel with uniform axial density immediately after the particles are trapped show that the bunch is accelerated to high energy while preserving its low momentum spread (Fig. 7). Because the bunch is short compared to the plasma wavelength, it sees a nearly even accelerating field and its momentum spread is nearly preserved as it accelerates in the channel, producing 0.2 MeV/c class momentum spread at high energy. These simulations have so far shown acceleration to beyond 20 MeV/c (limited by computational time) with 0.18 MeV/c longitudinal and 0.15 MeV/c transverse momentum spread, corresponding to $< 1\%$ energy spread and < 10 mrad divergence. Longer and 3D simulations using the envelope model are in progress to optimize bunch quality. Related simulations [28, 29] indicate that such post-acceleration nearly preserves absolute momentum spread, which may enable bunches at GeV energies and beyond with $< 0.1\%$ energy spread.

Accurate modeling of bunch momentum spread is required to simulate and design stages to post-accelerate low emittance bunches. Numerical work has shown that high order spline weighting of particle currents and forces to the grid reduces momentum errors [30]. The errors arise from discretization (of grid and macroparticles) and from interpolation of forces from the grid, and can lead to momentum and orbit displacements that introduce unphysical momentum spread. High order weight combined with digital smoothing of current deposition also suppressed numerical heating which can cause further error. The impact of these methods on bunch momentum spread accuracy has been characterized by benchmarking runs conducted with various weighting and smoothing functions to 2004 experiments producing 100 MeV self-trapped bunches [4], and by convergence testing each method with resolution [31]. Use of third order particle weighting and smoothing reduced unphysical growth of bunch transverse momentum and divergence at least tenfold, greatly improving kinetic accuracy with only fraction-

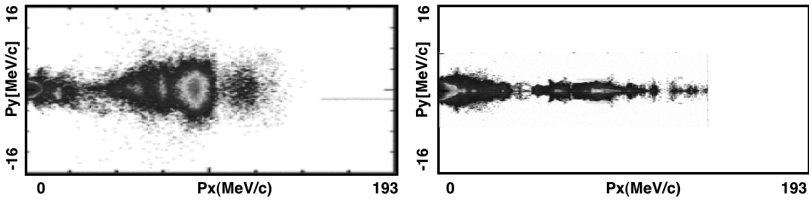

FIGURE 8. (color). The Px-Py (longitudinal vs. transverse momentum) phase space for two runs modeling 100 MeV-class experiments. Using standard first order particle weighting (left), divergence (Py/Px) is much greater than experiments, while using third order weighting with smoothing produced divergence matching the experiment.

ally increased runtime. Grid particle loaders and accurate laser launchers were also used to avoid seeding unphysical asymmetry. Simulated divergence in the axis orthogonal to the laser polarization is $\sim$ 4-6 mrad FWHM using these techniques, in good agreement with the experimental observation of 3 mrad (Fig. 8, right). In contrast, improvement was slow with increased resolution when using first order weighting, at a cost O[resolution^4] in 2D (O[resolution^5] in 3D) for all spatial dimensions, time, and particles, emphasizing the importance of these techniques. Dispersive properties were not noticeably changed. These models are now being applied to design of low emittance stages.

In conclusion, experiments demonstrated that plasma gradient control of injection in LWFAs produced bunches with 10- to 100- fold lower momentum spread and variation than previous laser accelerators, and demonstrated day-to-day stability over a week of run time. The bunches displayed central momentum stability of 0.76$\pm$0.02 MeV/c, momentum spread in the longitudinal (transverse) direction of 0.17 (0.02) MeV/c FWHM, and pointing stability of 2 mrad or 0.002 MeV/c RMS. Charge stability between 15 and 45% RMS was observed, and normalized bunch emittance was inferred to be on the order of $0.2-0.4\pi$ mm-mrad, a ten-fold improvement over previous LWFAs. Simulations benchmarked to the experiments showed that by coupling these bunches to subsequent LWFAs, their low absolute momentum spread was preserved as the bunch accelerated, resulting in high energy beams with 0.2 MeV/c momentum spread and low emittance. This may allow bunches at GeV energies and beyond with $<$ 0.1% energy spread. Simulation techniques including high order particle weight were shown to suppress momentum errors, allowing accurate modeling of post-acceleration stages to maintain the low momentum spread and emittance generated to high energies. Together with the observed stability over many run days, these properties will benefit many LWFA applications.

ACKNOWLEDGMENTS

Work supported by the U.S. Dept. of Energy contracts DE-AC02-05CH11231, DE-FC02-07ER41499, DE-FG02-06ER84484, DE-FG03-95ER40926, DE-FG02-01ER41178, DE-FG02-03ER83857, DOE SciDAC, NERSC, and ATLAS programs, NSF 0113907 and 0614001, and DARPA. We appreciate the contributions of J. van Tilborg, D. Panasenko, K. Paul, P. Mullowney, P. Messmer, V. Leurent, S.A. Gaillard,

D. Syversrud, J. Wallig, N. Ybarrolaza, and the VORPAL development team.

REFERENCES

1. T. Tajima, and J. M. Dawson, *Phys. Rev. Lett.* **43**, 267–70 (1979).
2. W. P. Leemans, B. Nagler, A. J. Gonsalves, C. Tóth, K. Nakamura, C. G. R. Geddes, E. Esarey, C. B. Schroeder, and S. M. Hooker, *Nature Physics* **2**, 696–699 (2006).
3. E. Esarey, P. Sprangle, J. Krall, and A. Ting, *IEEE Trans. Plasma Sci.* **24**, 252–288 (1996).
4. C. G. R. Geddes, Cs. Tóth, J. van Tilborg, E. Esarey, C. B. Schroeder, D. Bruhwiler, C. Nieter, J. Cary, and W. P. Leemans, *Nature* **431**, 538–541 (2004).
5. S. P. D. Mangles, C. Murphy, Z. Najmudin, A. Thomas, J. Collier, A. Dangor, E. Divali, P. Foster, J. Gallacher, C. Hooker, D. Jaroszynski, A. Langley, W. Mori, P. Norreys, F. Tsung, R. Viskup, B. Walton, and K. Krushelnick, *Nature* **431**, 535–538 (2004).
6. J. Faure, Y. Glinec, A. Pukhov, S. Kiselev, S. Gordienko, E. Lefebvre, J.-P. Rousseau, F. Burgy, and V. Malka, *Nature* **431**, 541–544 (2004).
7. K. Nakamura, B. Nagler, C. Tóth, C. G. R. Geddes, C. B. Schroeder, E. Esarey, W. P. Leemans, A. Gonsalves, and S. Hooker, *Phys. Plasmas* **14**, 056708 (2007).
8. C. G. R. Geddes, Cs. Tóth, J. van Tilborg, E. Esarey, C. B. Schroeder, D. Bruhwiler, C. Nieter, J. Cary, and W. P. Leemans, *Phys. Plasmas* **12**, 056709 (2005).
9. C.-T. Hsieh, C.-M. Huang, C.-L. Chang, Y.-C. Ho, Y.-S. Chen, J.-Y. Lin, J. Wang, and S.-Y. Chen, *Phys. Rev. Lett.* **96**, 095001 (2006).
10. J. Faure, C. Rechatin, A. Norlin, A. Lifschitz, Y. Glinec, and V. Malka, *Nature* **444**, 737–739 (2006).
11. E. Esarey, R. F. Hubbard, W. P. Leemans, A. Ting, and P. Sprangle, *Phys. Rev. Lett.* **79**, 2682–2685 (1997).
12. G. Fubiani, E. Esarey, C. B. Schroeder, and W. P. Leemans, *Phys. Rev. E* **70**, 016402 (2004).
13. H. Kotaki, S. Masuda, M. Kando, J. K. Koga, and K. Nakajima, *Phys. Plasmas* **11**, 3296–3302 (2004).
14. S. Bulanov, N. Naumova, F.Pegoraro, and J. Sakai, *Phys. Rev. E* **58**, R5257 (1998).
15. R. G. Hemker, N. M. Hafz, and M. Uesaka, *Phys. Rev. ST-AB* **5**, 041301 (2002).
16. H. Suk, N. Barov, J. B. Rosenzweig, and E. Esarey, *Phys. Rev. Lett.* **86**, 1011 (2001).
17. V. Petrillo, L. Serafini, and P. Tomassini, *Phys. Rev. ST-AB* **11**, 070703/1–7 (2008).
18. C. G. R. Geddes, K. Nakamura, G. R. Plateau, Cs. Tóth, E. Cormier-Michel, E. Esarey, C. B. Schroeder, J. Cary, and W. P. Leemans, *Phys. Rev. Lett.* **100**, 215004 (2008).
19. LOASIS facility: http://loasis.lbl.gov/ (LBNL).
20. For BPS data, a second laser pulse (2 TW) was present from other experiments. Bunch properties were independent of its pointing. Spectrometer data (no second laser), verified the second laser did not affect the bunch.
21. C. G. R. Geddes, Cs. Tóth, J. van Tilborg, E. Esarey, C. B. Schroeder, J. Cary, and W. P. Leemans, *Phys. Rev. Lett.* **95**, 145002 (2005).
22. C. Nieter, and J. Cary, *J. Comp. Phys.* **196**, 448–473 (2004).
23. P. Messmer, and D. L. Bruhwiler, *Phys. Rev. ST Accel. Beams* **9**, 031302 (2006).
24. B. Cowan, D. Bruhwiler, P. Messmer, K. Paul, C. Geddes, E. Esarey, and E. Cormier-Michel, "Laser wakefield simulation using a speed-of-light frame envelope model," in these proceedings.
25. C. G. R. Geddes, *Plasma Channel Guided Laser Wakefield Accelerator*, Ph.D. dissertation, University of California, Berkeley, Berkeley CA, 2005.
26. F. S. Tsung, R. Narang, W. B. Mori, C. Joshi, R. A. Fonseca, and L. O. Silva, *Phys. Rev. Lett.* **93**, 185002 (2004).
27. G. Plateau, E. Esarey, C. G. R. Geddes, W. P. Leemans, N. Matlis, C. B. Schroeder, J. van Tilborg, and Cs. Tóth, "Recent progress at LBNL on characterization of laser wakefield accelerated electron bunches using coherent transition radiation," in *Proc. Part. Accel. Conf.*, IEEE, Piscataway, NJ, 2007.
28. N. E. Andreev, S. V. Kuznetsov, and I. V. Pogorelsky, *Phys. Rev. ST-AB* **3**, 021301 (2000).
29. B. A. Shadwick (2005), private communication.
30. E. Cormier-Michel, B. A. Shadwick, C. G. R. Geddes, E. Esarey, C. B. Schroeder, and W. P. Leemans, *Phys. Rev. E* **78**, 016404 (2008).
31. D. Bruhwiler, and et al, *in preparation* (2008).